## Supplementary material

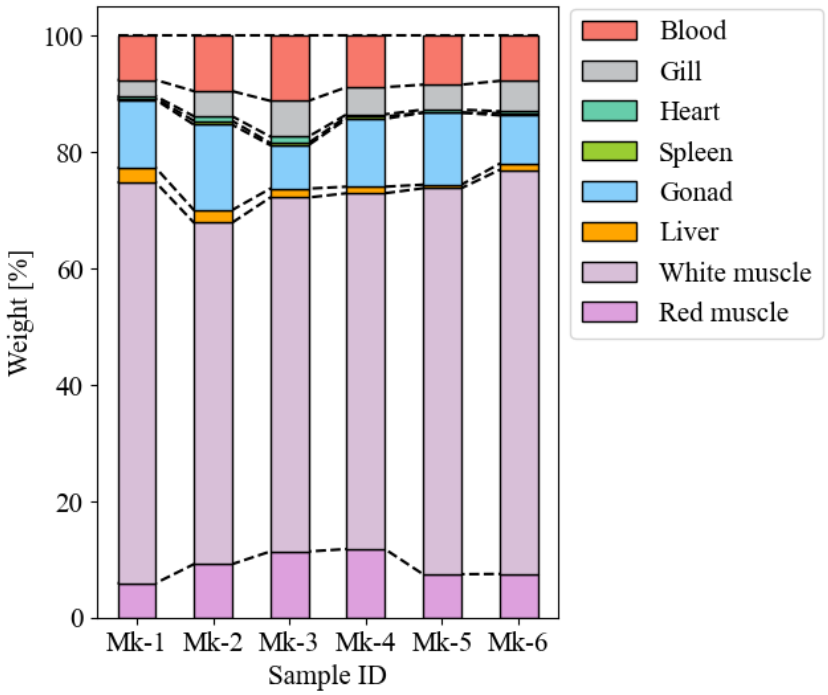


**Figure S1: Proportion of wet weight among chub mackerel tissues.**

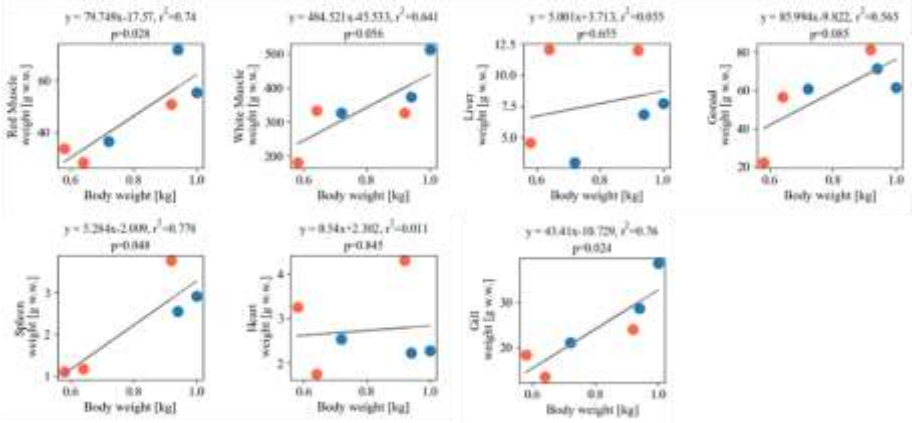


**Figure S2: Correlation between tissue weight and total body weight. Red circles represent females, and blue circles represent males. Black lines show the linear regression of all data points.**

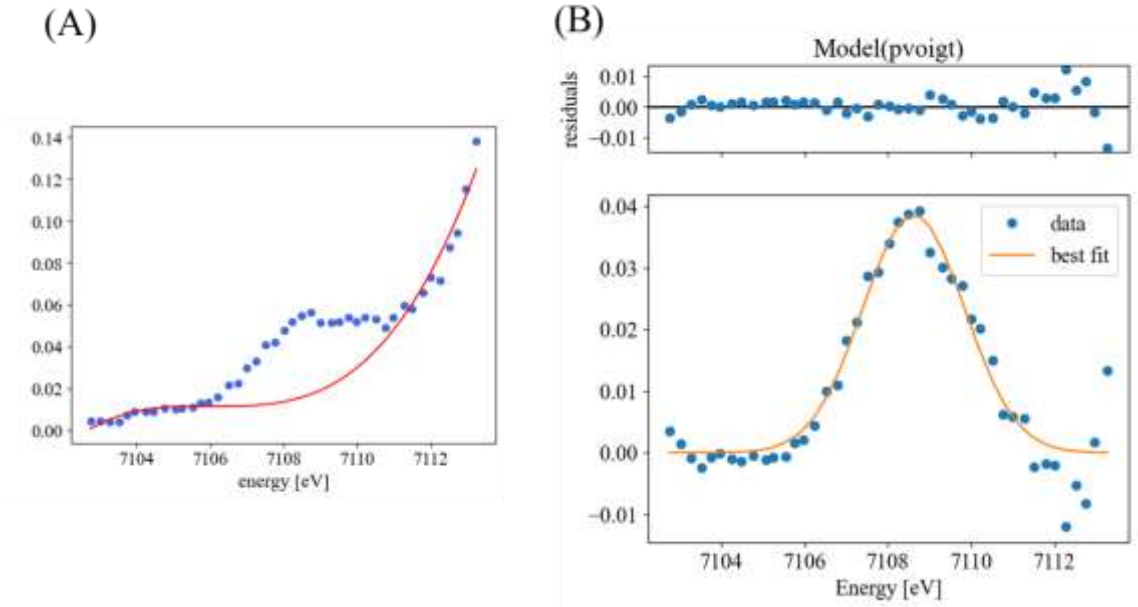


**Figure S3: Example of pre-edge curve fitting. Blue dotes in panel (A) represent the raw spectra around the pre-edge peak. The red line is a spline curve fitted to the raw spectra excluding the pre-edge region. The dotes in panel (B) show the data obrained by subtracting the spline curve from the raw spectra. The orange line represents the fitted pseudo-Voigt model.**

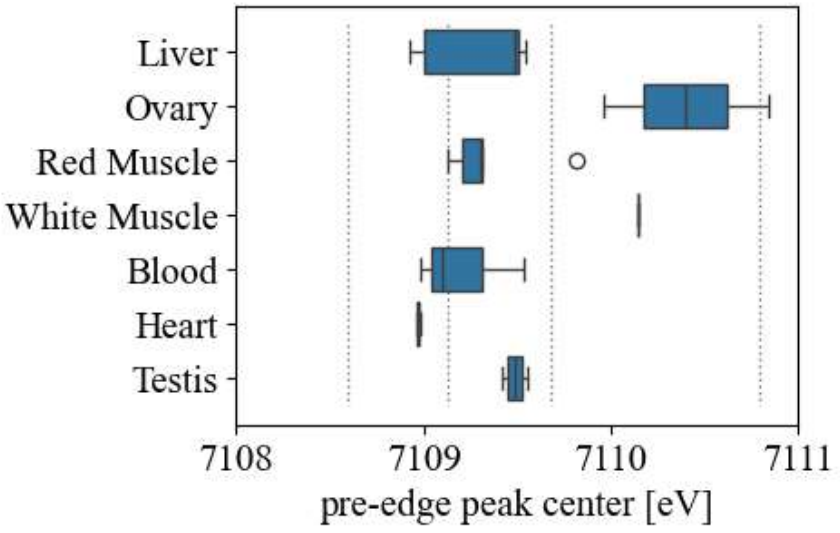


**Figure S4: Pre-edge peak energies in the spectra of chub mackerel tissues. Gray dotted lines indicate the values for the following standard materials: horse spleen ferritin (Hs-Ft; 7110.8 eV), bovine blood methemoglobin (Bb-metHb; 7109.7 eV), bovine blood oxyhemoglobin (Bb-oxyHb; 7109.1 eV), and bovine deoxyhemoglobin (Bb-deoxyHb; 7108.6 eV)**

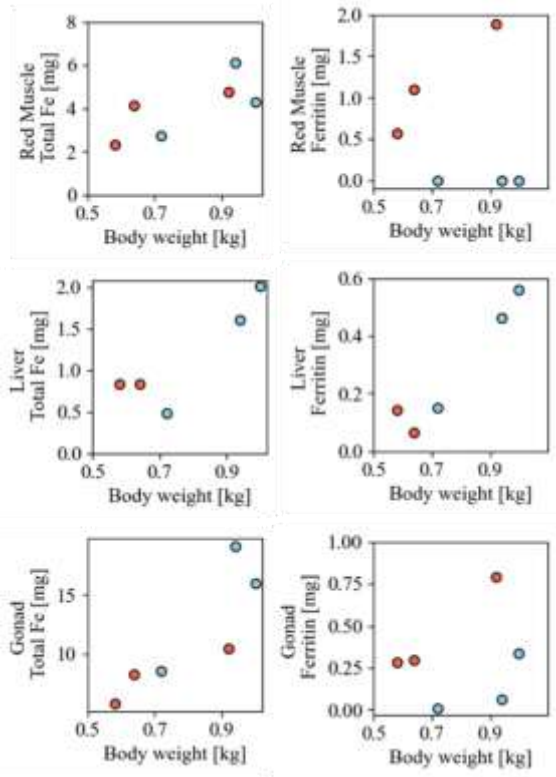


**Figure S5: Correlations between body weights and iron content in either the total tissue compartment or the ferritin reservoir. Red circles represent females, and blue circles represent males.**

**Table S1: Tissue wet weights (g) of chub mackerel.**

| Sample ID | Mk-1 | Mk-2 | Mk-3 | Mk-4 | Mk-5 | Mk-6 | Mean |
|---|---|---|---|---|---|---|---|
| All internal organs | 106 | 131 | 73 | 128 | 120 | 127 | 114 |
| Red muscle | 31.1 | 52.7 | 36.5 | 73.8 | 39.1 | 57.7 | 48.5 |
| White muscle | 333 | 326 | 182 | 374 | 326 | 513 | 342 |
| Liver | 13.7 | 13.6 | 6.1 | 10.1 | 5.3 | 10.6 | 9.90 |
| Ovary | 58.6 | 84.3 | 23.7 | NA | NA | NA | 55.5 |
| Testis | NA | NA | NA | 75.7 | 65.7 | 67.6 | 69.7 |
| Spleen | 2.7 | 4.8 | 2.8 | 5 | NA | 5.2 | 4.10 |
| Heart | 4 | 5.6 | 5.1 | 4.6 | 5.6 | 3.5 | 4.73 |
| Blood | 5.1 | 4.6 | 1.8 | 5.5 | 6.1 | 12.5 | 5.93 |
| Gill | 14.7 | 25.6 | NA | 31 | 21.1 | 40.9 | 26.7 |
| Gut | 25.2 | 31.5 | 32.3 | 29.5 | 25.2 | 42.4 | 31.0 |
| Carcass | 161 | 386 | 278 | 299 | 174 | 270 | 261 |

**Table S2: Iron concentrations, amounts, and stable isotope ratios in tissues of chub mackerel.**

| Sample ID | Tissue | $\delta^{56}$Fe ± 2 S.E. | Fe conc. [µg/g w.w.] | Fe conc. [µg/g d.w.] | Total Fe [mg] |
|---|---|---|---|---|---|
| Mk-1 | Red Muscle | − 1.5 ± 0.05 | 144.36 | 317.57 | 4.12 |
| Mk-1 | White Muscle | − 1.39 ± 0.05 | 4.01 | 12.18 | 1.33 |
| Mk-1 | Liver | − 1.21 ± 0.04 | 68.95 | 283.11 | 0.83 |
| Mk-1 | Gonad | − 1.48 ± 0.09 | 9.34 | 22.38 | 0.53 |
| Mk-1 | Spleen | − 1.26 ± 0.04 | 720.77 | 3210.5 | 0.85 |
| Mk-1 | Heart | − 1.4 ± 0.05 | 120.72 | 569.19 | 0.21 |
| Mk-1 | Blood | − 1.29 ± 0.04 | 222.27 | 1201.54 | 8.29 |
| Mk-1 | Gill | − 1.2 ± 0.01 | 96.15 | 329.5 | 1.3 |
| Mk-2 | Red Muscle | − 1.56 ± 0.03 | 93.45 | 194.25 | 4.77 |
| Mk-2 | White Muscle | − 1.5 ± 0.04 | 4.5 | 10.36 | 1.47 |
| Mk-2 | Liver | − 1.25 ± 0.002 | 80.49 | 342.72 | 0.97 |
| Mk-2 | Gonad | − 1.21 ± 0.06 | 12.32 | 26.03 | 1 |
| Mk-2 | Spleen | − 1.46 ± 0.04 | 431 | 2306.69 | 1.62 |
| Mk-2 | Heart | − 1.51 ± 0.06 | 70.43 | 393.93 | 0.3 |
| Mk-2 | Blood | − 1.42 ± 0.04 | 196.19 | 1105.47 | 10.51 |
| Mk-2 | Gill | − 1.34 ± 0.07 | 63.07 | 228.04 | 1.51 |
| Mk-3 | Red Muscle | − 1.53 ± 0.04 | 68.94 | 279.89 | 2.34 |
| Mk-3 | White Muscle | − 1.53 ± 0.04 | 4.77 | 20.29 | 0.87 |
| Mk-3 | Liver | − 1.2 ± 0.04 | 181.92 | 695.04 | 0.83 |
| Mk-3 | Gonad | − 1.5 ± 0.06 | 16.08 | 46.54 | 0.36 |
| Mk-3 | Spleen | − 1.39 ± 0.04 | 891.42 | 3178.31 | 0.99 |
| Mk-3 | Heart | − 1.42 ± 0.04 | 262.33 | 1283.99 | 0.86 |
| Mk-3 | Blood | − 1.39 ± 0.03 | 174.24 | 1085.33 | 5.89 |
| Mk-3 | Gill | − 1.43 ± 0.04 | 73.61 | 324.04 | 1.35 |
| Mk-4 | Red Muscle | − 1.66 ± 0.04 | 84.66 | 217.74 | 6.09 |
| Mk-4 | White Muscle | − 1.58 ± 0.03 | 3.64 | 12.44 | 1.36 |
| Mk-4 | Liver | − 1.07 ± 0.04 | 234.24 | 858.21 | 1.61 |
| Mk-4 | Gonad | − 1.04 ± 0.06 | 10.68 | 47.63 | 0.76 |
| Mk-4 | Spleen | − 1.43 ± 0.04 | 872.5 | 3425.53 | 2.22 |
| Mk-4 | Heart | − 1.49 ± 0.03 | 120.75 | 516.76 | 0.27 |
| Mk-4 | Blood | − 1.28 ± 0.05 | 349.12 | 1704.59 | 19.12 |
| Mk-4 | Gill | − 1.37 ± 0.04 | 68.96 | 253.94 | 1.97 |

**Table S2: Continued.**

| Sample ID | Tissue | $\delta^{56}$Fe ± 2 S.E. | Fe conc. [µg/g w.w.] | Fe conc. [µg/g d.w.] | Total Fe [mg] |
|---|---|---|---|---|---|
| Mk-5 | Red Muscle | − 1.36 ± 0.05 | 74.99 | 279.26 | 2.75 |
| Mk-5 | White Muscle | − 1.26 ± 0.08 | 6.28 | 23.29 | 2.05 |
| Mk-5 | Liver | − 1.3 ± 0.05 | 161.98 | 615.63 | 0.49 |
| Mk-5 | Gonad | − 1.26 ± 0.03 | 5.29 | 26.83 | 0.32 |
| Mk-5 | Spleen | NA | NA | NA | NA |
| Mk-5 | Heart | − 1.24 ± 0.06 | 144.24 | 676.72 | 0.37 |
| Mk-5 | Blood | − 1.4 ± 0.06 | 206.17 | 1038.39 | 8.65 |
| Mk-5 | Gill | − 1.34 ± 0.04 | 65.12 | 262.66 | 1.37 |
| Mk-6 | Red Muscle | − 1.65 ± 0.05 | 77.27 | 233.16 | 4.28 |
| Mk-6 | White Muscle | − 1.47 ± 0.05 | 3.85 | 13.17 | 1.98 |
| Mk-6 | Liver | − 1.11 ± 0.05 | 259.06 | 992.82 | 2.01 |
| Mk-6 | Gonad | − 0.92 ± 0.0001 | 9.17 | 51.65 | 0.56 |
| Mk-6 | Spleen | − 1.3 ± 0.05 | 875.43 | 3531.84 | 2.56 |
| Mk-6 | Heart | − 1.53 ± 0.05 | 185.29 | 865.38 | 0.42 |
| Mk-6 | Blood | − 1.58 ± 0.04 | 275 | 1480.91 | 16.02 |
| Mk-6 | Gill | − 1.56 ± 0.05 | 94.75 | 349.44 | 3.65 |

**Principal Component Analysis of XANES**

Evaluation by Linear combination fitting (LCF) carries the risk of incorrectly identifying components not originally present in the sample when too many components are included in the fitting. To address this, the number of contributing components was determined using principal component analysis (PCA) and target transformation analysis, as described by (Ressler et al., 2000) and (Martini et al., 2020). PCA of XANES spectra was performed using the singular value decomposition (SVD) algorithm, expressed as follows:

$$[A] = [E] \cdot [V] \cdot [w]^t \qquad (S-1)$$

This means that any m × n matrix A (where m ≥ n) can be decomposed into the product of an m × n column-orthogonal matrix E, an n × n diagonal matrix V, and the transpose of an n × n orthogonal matrix w. The matrix A was constructed so that each column represented a sample XANES spectrum interpolated onto the same energy grid. The singular values, represented by the diagonal elements of V, were determined so that the experimental spectra can be reconstructed by the minimal number of components which is equal to the principal component. The singular values of SVD results for the XANES spectra of the mackerel tissue samples indicated that approximately three to four components were sufficient to reconstruct the spectra (Figure S6).

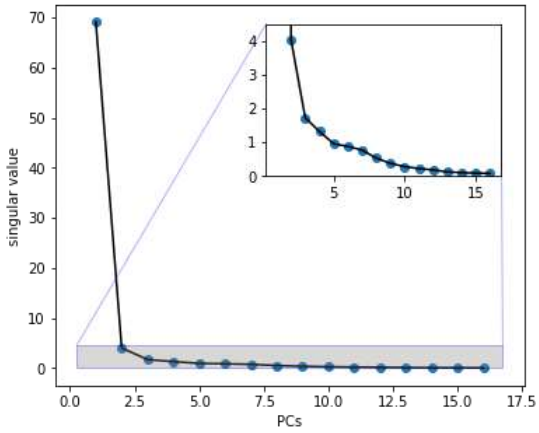


**Figure S6: SVD result of the tissue spectra.**

Next, sample spectra were reconstructed using one to three singular values from matrix V, as expressed as:

$$[E] \cdot [V^*] \cdot [w]^t = [A^*] \qquad (S-2)$$

where the matrix $A^*$ represents the reconstructed sample spectra, and $V^*$ is an n × n diagonal matrix whose diagonal elements consist of a selected subset of elements from V. For example, if two singular values are sufficient for reconstruction, $V^*$ is given by:

$$[V^*] = \begin{bmatrix} v_{11} & 0 & 0 & \cdots & 0 \\ 0 & v_{22} & 0 & \cdots & 0 \\ 0 & 0 & 0 & \cdots & 0 \\ \vdots & \vdots & \vdots & \vdots & \vdots \\ 0 & 0 & 0 & \cdots & 0 \end{bmatrix} \qquad (S-3)$$

The reconstructed spectra of fish tissue samples are shown in Figure B. The results indicate subtle differences between the original sample spectra and the reconstructed spectra when using $V^*$ with only one or two singular values (i.e. one or two

principal components), whereas using three principal components reproduces the sample spectra accurately (Figure S7).

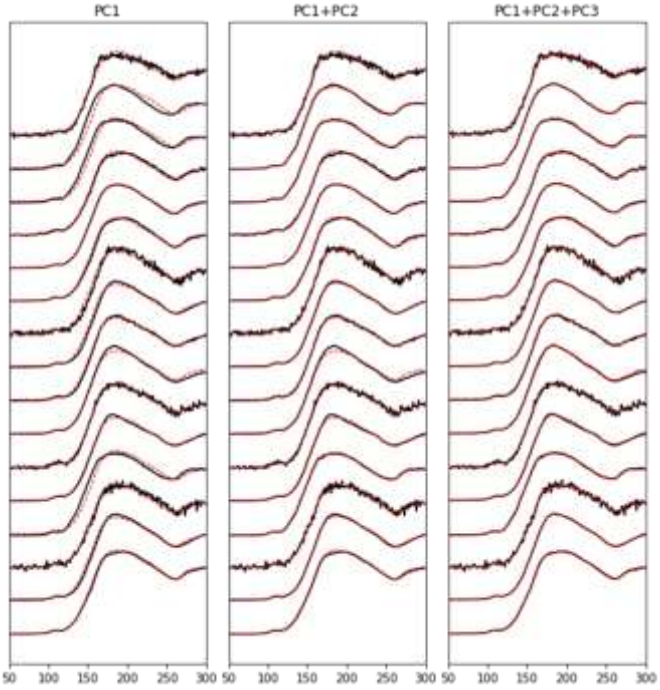


**Figure S7: Reconstructed sample spectra from PCA results. Black lines represent the measured spectra, and red lines represent the reconstructed spectra.**

To identify the standard materials that best fit the sample spectra, target transformation analysis was conducted. This analysis uses matrix E from the SVD results as follows:

$$[T^*] = [E] \cdot [E]^t \cdot [T] \qquad (S-4)$$

where T is a vector constructed from the XANES spectrum of standard materials. If the reconstructed vector $T^*$ closely matches T within experimental error, T is confirmed as a principal component of the sample spectra A. The target transformation results for various standard materials (Hs-ferritin, Bb-metHb, Bb-oxyHb, Bb-deoxyHb, $Fe_3O_4$, ferrihydrite, FeS, and hematite) are shown in Figure S8. These results indicated that ferritin and hemoglobin derivatives were principal components of the sample spectra, while other materials were not well reproduced. Because ferritin contains ferrihydrite-like nanoparticles within its cavity (Harrison et al., 1967; Theil, 1987), the similarity between the XANES spectra of ferritin and ferrihydrite allows for accurate reconstruction of the ferrihydrite spectrum from the sample spectra.

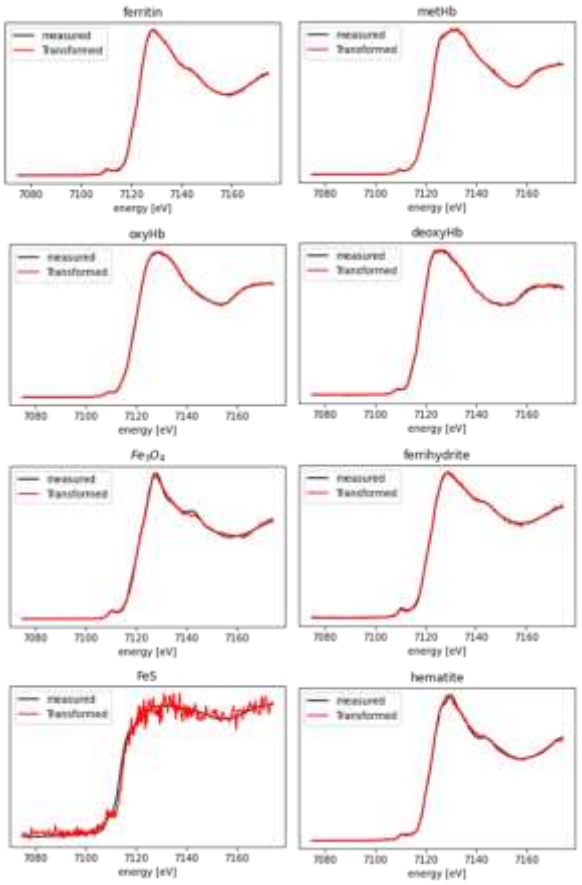


**Figure S8: Results of target transformation of standard materials. Black lines represent the measured spectra, and red lines represent the transformed**

## References

Harrison, P. M., Fischbach, F. A., Hoy, T. G., and Haggis, G. H.: Ferric Oxyhydroxide Core of Ferritin, Nature, 216, 1188–1190, doi: 10.1038/2161188a0, 1967.

Martini, A., Guda, S. A., Guda, A. A., Smolentsev, G., Algasov, A., Usoltsev, O., Soldatov, M. A., Bugaev, A., Rusalev, Yu., Lamberti, C., and Soldatov, A. V.: PyFitit: The software for quantitative analysis of XANES spectra using machine-learning algorithms, Comput Phys Commun, 250, 107064, doi: 10.17632/ydkgfdc38t.1, 2020.

Ressler, T., Wong, J., Roos, J., and Smith, I. L.: Quantitative speciation of mn-bearing particulates emitted from autos burning (methylcyclopentadienyl) manganese tricarbonyl-added gasolines using XANES spectroscopy, Environ Sci Technol, 34, 950–958, doi: 10.1021/es990787x, 2000.

Theil, E. C.: Ferritin: structure, gene regulation, and cellular function in animals, plants, and microorganisms., Annu Rev Biochem, 56, 289–315, doi: 10.1146/annurev.bi.56.070187.001445, 1987.